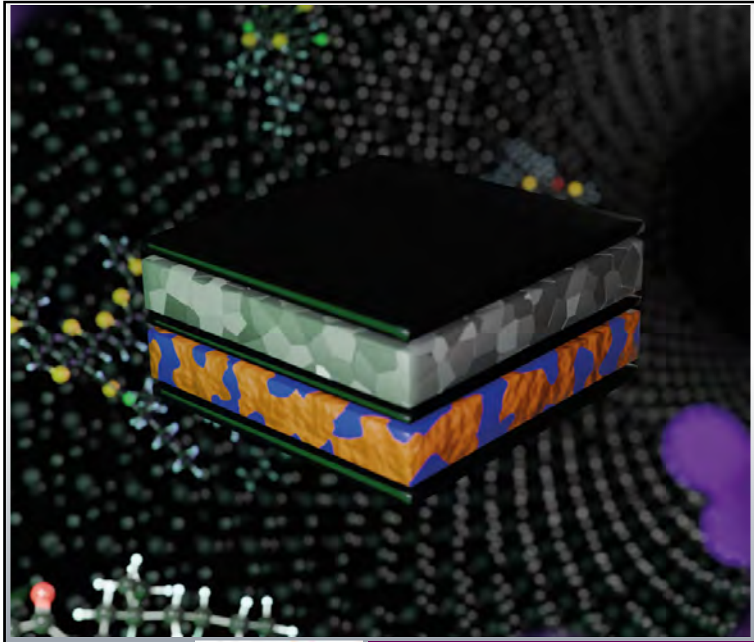

Scanning Thermal Microscopy of functional layers used in halide perovskite devices

Ralf Heiderhoff

School of Electrical, Information and Media Engineering
Institute of Electronic Devices
Summer School Khiva | May 2023

Introduction

University of Wuppertal

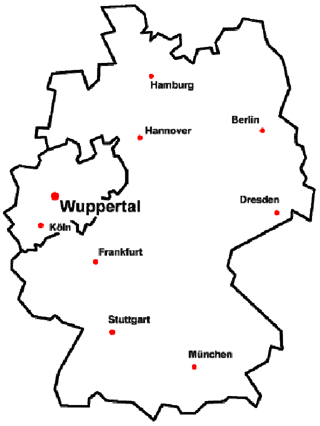

Germany

suspension railway

- since 1863 School of Engineering
- 1972 Foundation of BU Wuppertal
- 8 Faculties
- 24,000 Students

Introduction

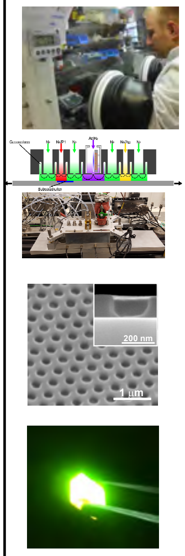

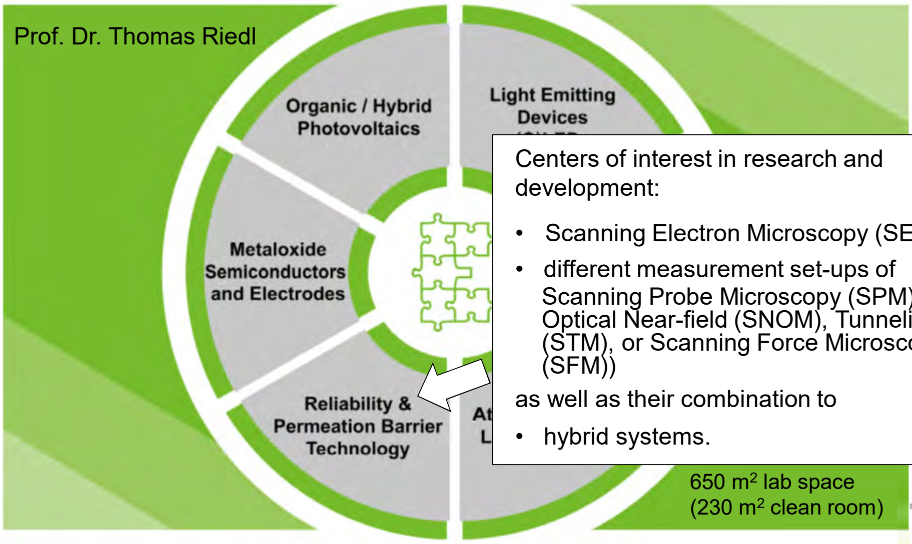

650 m² lab space
(230 m² clean room)

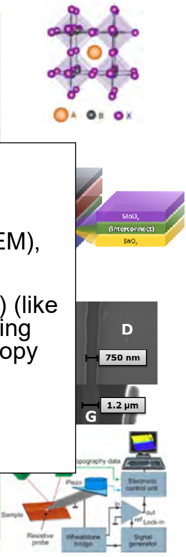

Centers of interest in research and development:

- Scanning Electron Microscopy (SEM),
- different measurement set-ups of Scanning Probe Microscopy (SPM) (like Optical Near-field (SNOM), Tunneling (STM), or Scanning Force Microscopy (SFM))

as well as their combination to

- hybrid systems.

Motivation and Purpose

Best Research-Cell Efficiencies

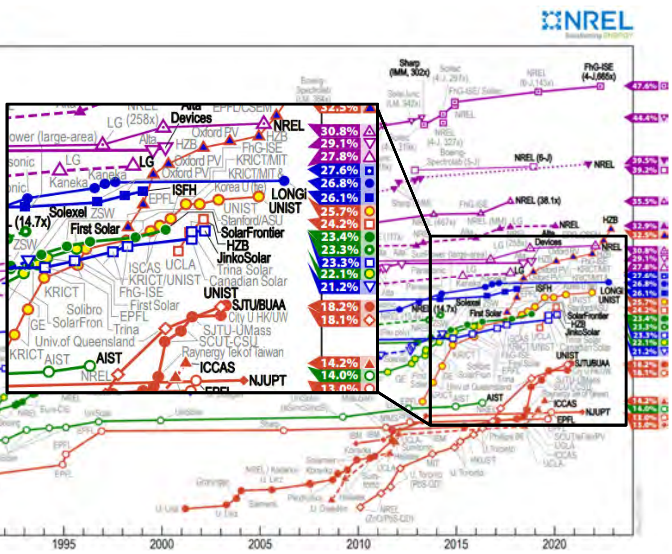

World record in solar cell research: Perovskite-organic tandem solar cells

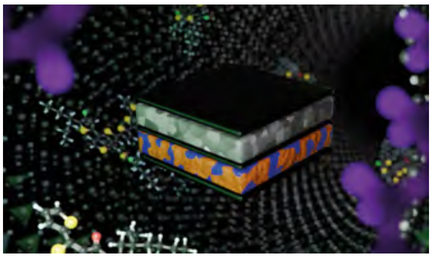

- next-generation (perovskite-organic) tandem solar cells reaching a new efficiency record of 24%
- published in Nature 604, 280 (2022)

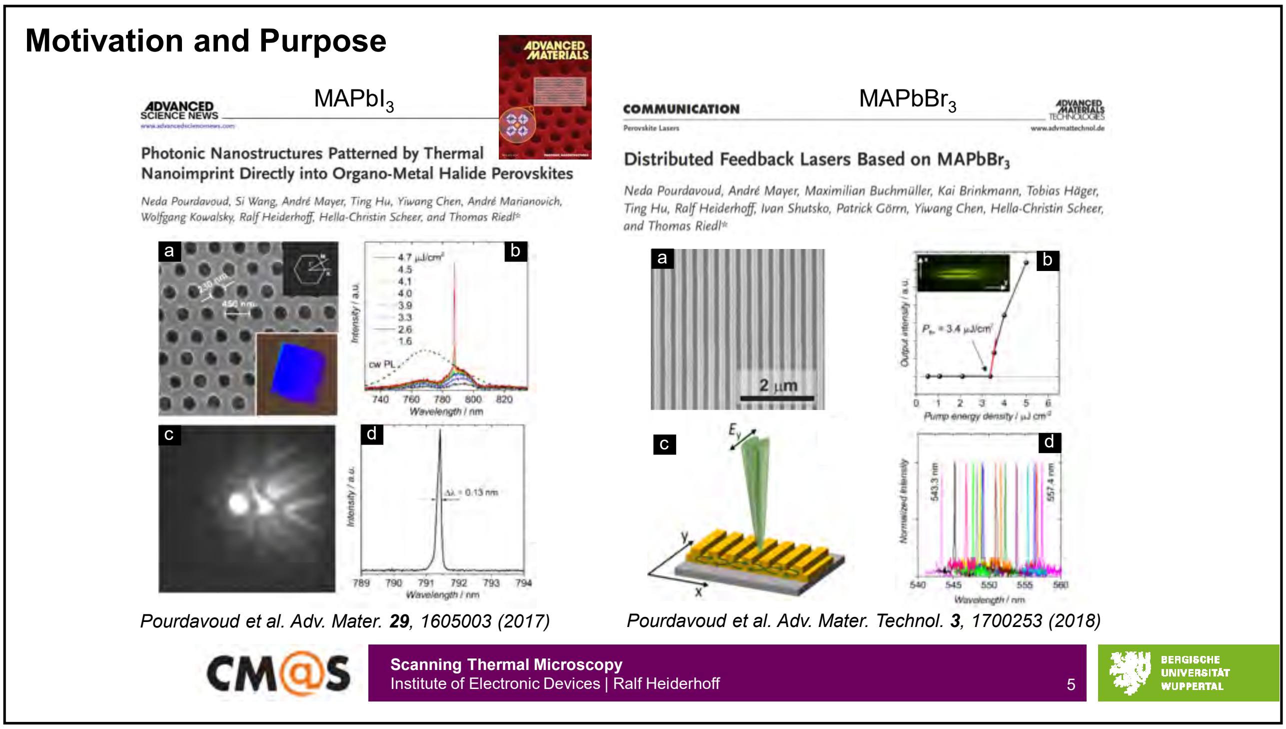

Motivation and Purpose

$MAPbI_3$

ADVANCED SCIENCE NEWS
www.advancedsciencenews.com

Photonic Nanostructures Patterned by Thermal Nanoimprint Directly into Organo-Metal Halide Perovskites

*Neda Pourdavoud, Si Wang, André Mayer, Ting Hu, Yiwang Chen, André Marianovich, Wolfgang Kowalsky, Ralf Heiderhoff, Hella-Christin Scheer, and Thomas Riedl**

Pourdavoud et al. *Adv. Mater.* **29**, 1605003 (2017)

$MAPbBr_3$

COMMUNICATION
Perovskite Lasers

ADVANCED MATERIALS TECHNOLOGIES
www.advmattechnol.de

Distributed Feedback Lasers Based on $MAPbBr_3$

*Neda Pourdavoud, André Mayer, Maximilian Buchmüller, Kai Brinkmann, Tobias Häger, Ting Hu, Ralf Heiderhoff, Ivan Shutsko, Patrick Görrn, Yiwang Chen, Hella-Christin Scheer, and Thomas Riedl**

Pourdavoud et al. *Adv. Mater. Technol.* **3**, 1700253 (2018)

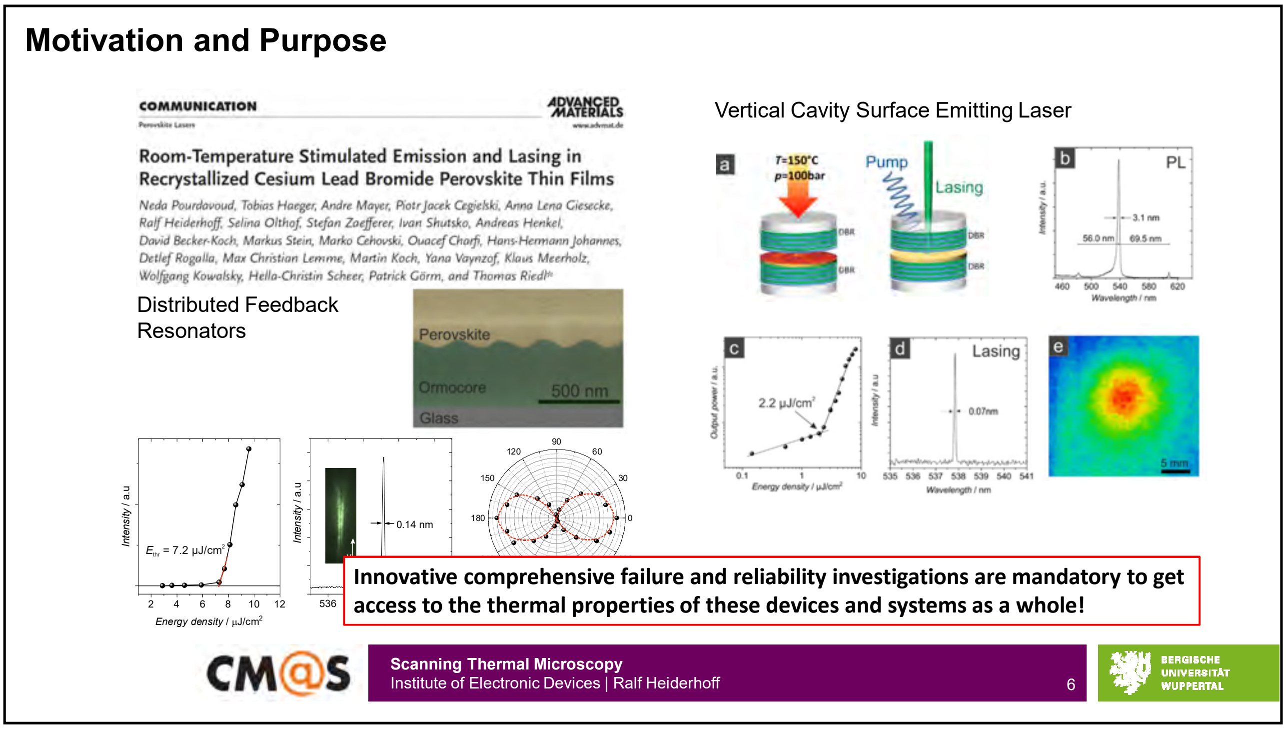

Motivation and Purpose

COMMUNICATION
Perovskite Lasers

ADVANCED MATERIALS
www.advmat.de

Room-Temperature Stimulated Emission and Lasing in Recrystallized Cesium Lead Bromide Perovskite Thin Films

*Neda Pourdavoud, Tobias Haeger, Andre Mayer, Piotr Jacek Cegielski, Anna Lena Giesecke, Ralf Heiderhoff, Selina Olthof, Stefan Zaefferer, Ivan Shutsko, Andreas Henkel, David Becker-Koch, Markus Stein, Marko Cehovski, Ouacef Charfi, Hans-Hermann Johannes, Detlef Rogalla, Max Christian Lemme, Martin Koch, Yana Vaynzof, Klaus Meerholz, Wolfgang Kowalsky, Hella-Christin Scheer, Patrick Görrn, and Thomas Riedl**

Distributed Feedback Resonators

Vertical Cavity Surface Emitting Laser

Innovative comprehensive failure and reliability investigations are mandatory to get access to the thermal properties of these devices and systems as a whole!

Motivation

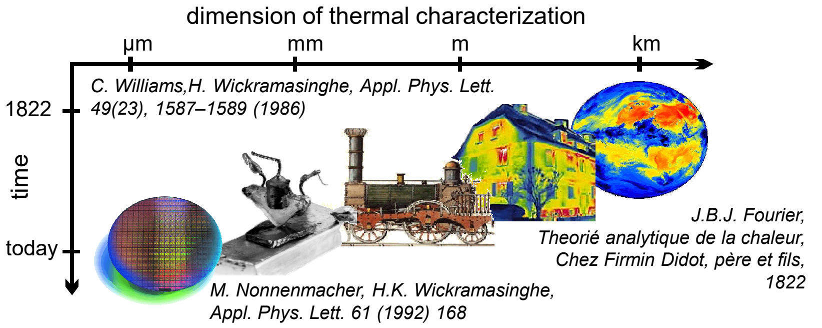

C. Williams,H. Wickramasinghe, Appl. Phys. Lett. 49(23), 1587–1589 (1986)

J.B.J. Fourier, Theorié analytique de la chaleur, Chez Firmin Didot, père et fils, 1822

M. Nonnenmacher, H.K. Wickramasinghe, Appl. Phys. Lett. 61 (1992) 168

Fourier law $\vec{q} = -\overleftrightarrow{\lambda} \cdot grad\, T(\vec{r})$

general equation of heat conduction
$$\rho c \frac{\partial T(\vec{r})}{\partial t} = \frac{\partial}{\partial x}\left(\lambda_x \frac{\partial T(\vec{r})}{\partial x}\right) + \frac{\partial}{\partial y}\left(\lambda_y \frac{\partial T(\vec{r})}{\partial y}\right) + \frac{\partial}{\partial z}\left(\lambda_z \frac{\partial T(\vec{r})}{\partial z}\right) + \dot{q}_E$$

ρ: specific density $\dot{q}_E$: amount of heat generated per unit time and unit volume

A. Freeman, Theory of heat, Cambridge University Press, London, 1878

Set-up of Scanning Thermal Microscope

P. Tovee et al.; Journal of Applied Physics, (2012) 112, 114317

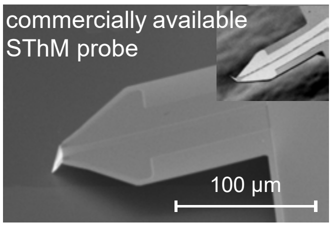

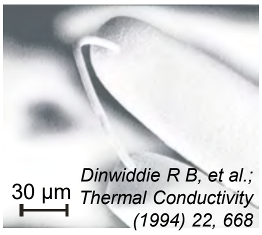

Dinwiddie R B, et al.; Thermal Conductivity (1994) 22, 668

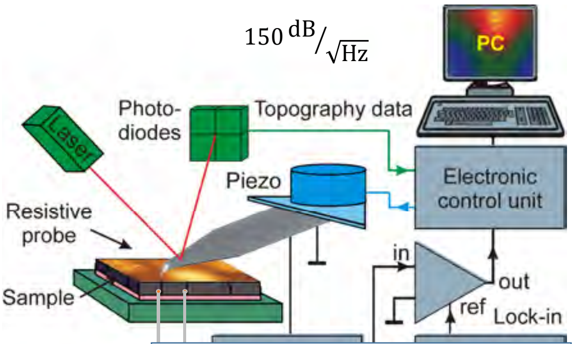

S. Huth, O. Breitenstein, A. Huber, D. Dantz, U. Lambert, F. Altmann, Solid State Phenom. 82-84 (2002) 741–746.

M. Ma

I. Joachimsthaler et al., Journal of Measurement Science and Technology 14, (2003), 87–96

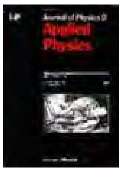

Measurements of temperature distributions

Voltage source:
local heat
dissipation in
dependence on
the heating power
density

*G.B.M. Fiege et al.
Microelectron. Reliab.
38 (1998) 957–961.*

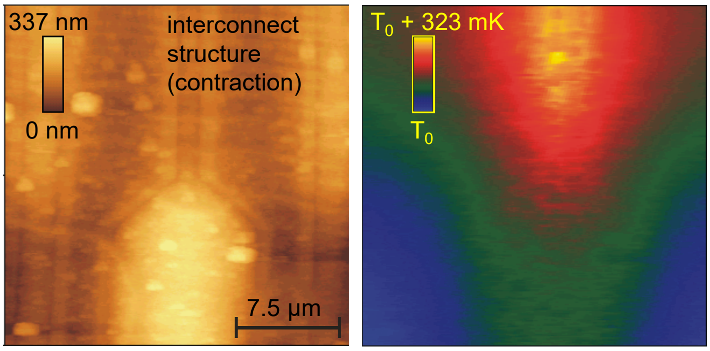

Topography Temperature

$5\,\frac{mK}{\sqrt{Hz}}$: thermal noise

$\frac{\Delta x}{\Delta T}$: 1/temperature gradient

$30\ nm$: effect. contact area in air

achievable spatial resolution:

$$\Delta x = 5\,\frac{mK}{}\cdot\sqrt{\Delta f}\,\frac{\Delta x}{} + 30\ nm$$

10 nm: in ultra high vaccuum
W. Jeong et al., Sci.Rep.4 (2014) 4975

Reliability investigations by means of SThM

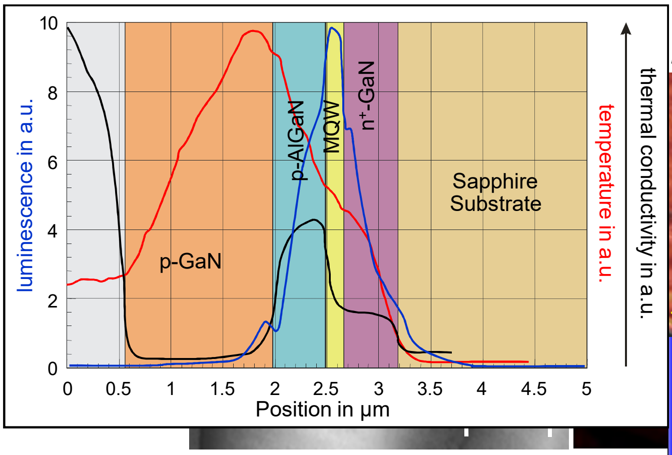

Topography

M. Palaniappan et al., Proc. 25th Int. Symp. Test. Fail. Ana

R. Heiderhoff et al., Microelectron. Reliab. 40 (2000) 1383–1388

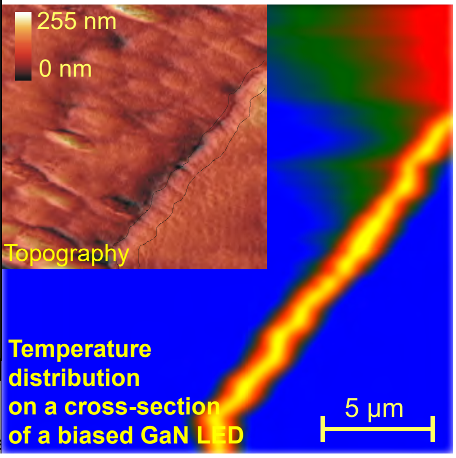

Temperature distribution on a cross-section of a biased GaN LED

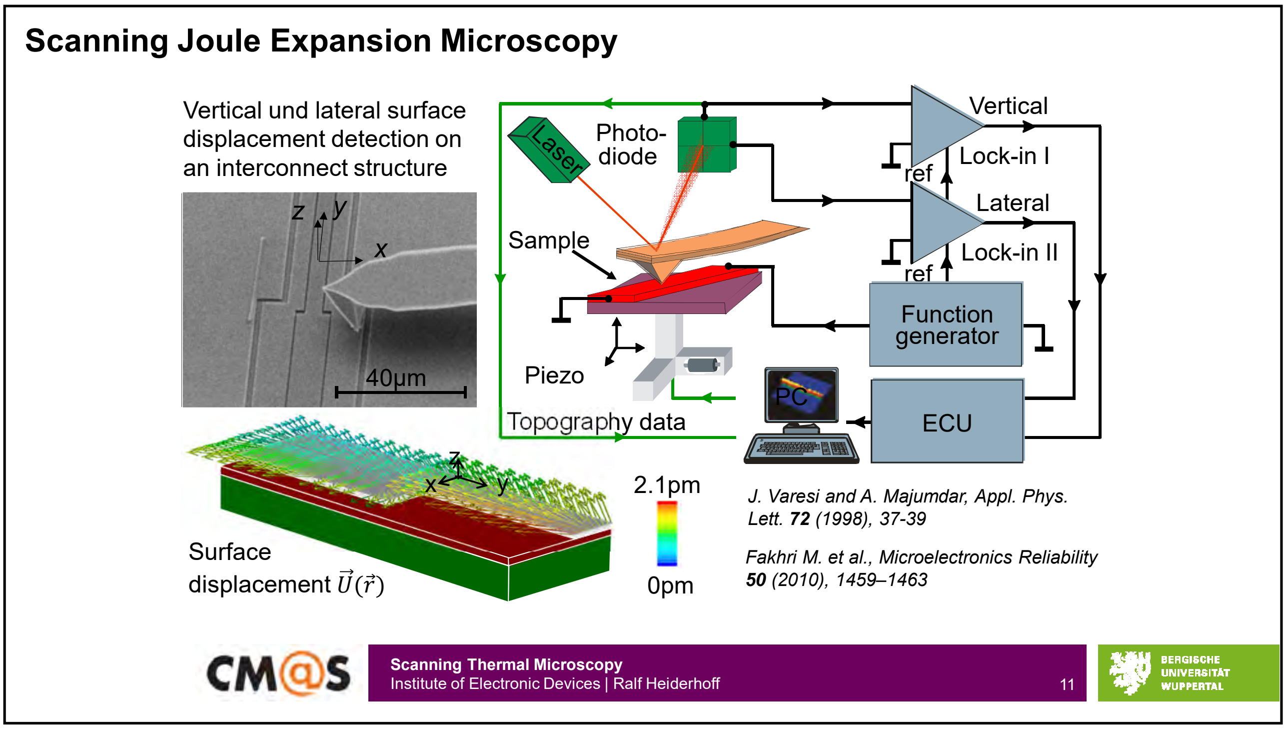

Scanning Joule Expansion Microscopy

Vertical und lateral surface displacement detection on an interconnect structure

Surface displacement $\vec{U}(\vec{r})$

J. Varesi and A. Majumdar, Appl. Phys. Lett. ***72*** *(1998), 37-39*

Fakhri M. et al., Microelectronics Reliability ***50*** *(2010), 1459–1463*

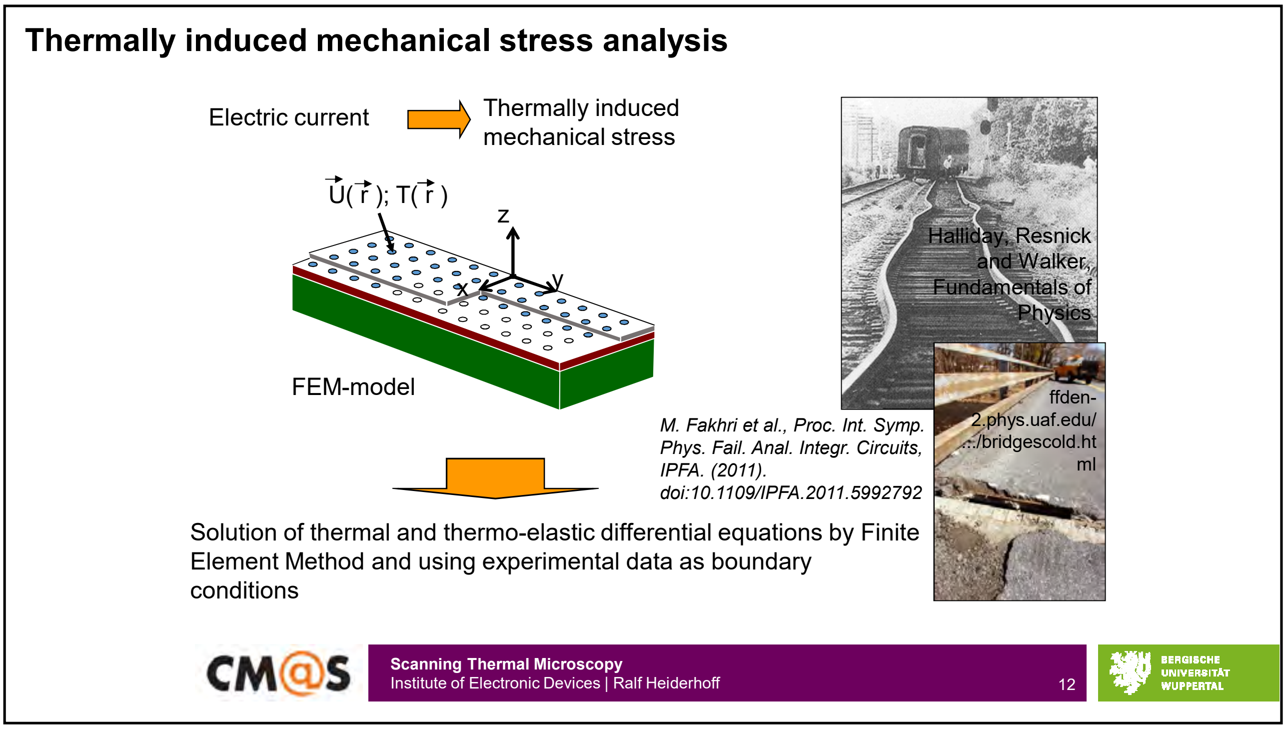

Thermally induced mechanical stress analysis

Electric current → Thermally induced mechanical stress

M. Fakhri et al., Proc. Int. Symp. Phys. Fail. Anal. Integr. Circuits, IPFA. (2011). doi:10.1109/IPFA.2011.5992792

Solution of thermal and thermo-elastic differential equations by Finite Element Method and using experimental data as boundary conditions

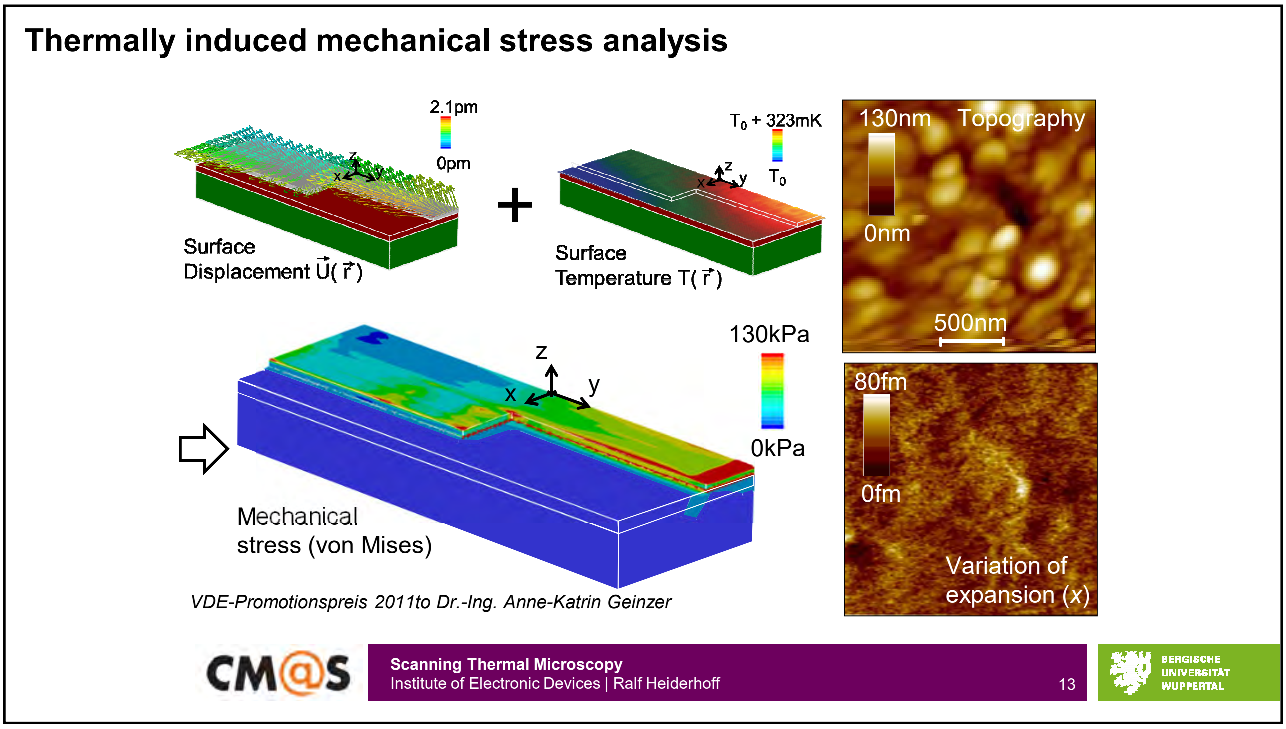

Thermally induced mechanical stress analysis

VDE-Promotionspreis 2011to Dr.-Ing. Anne-Katrin Geinzer

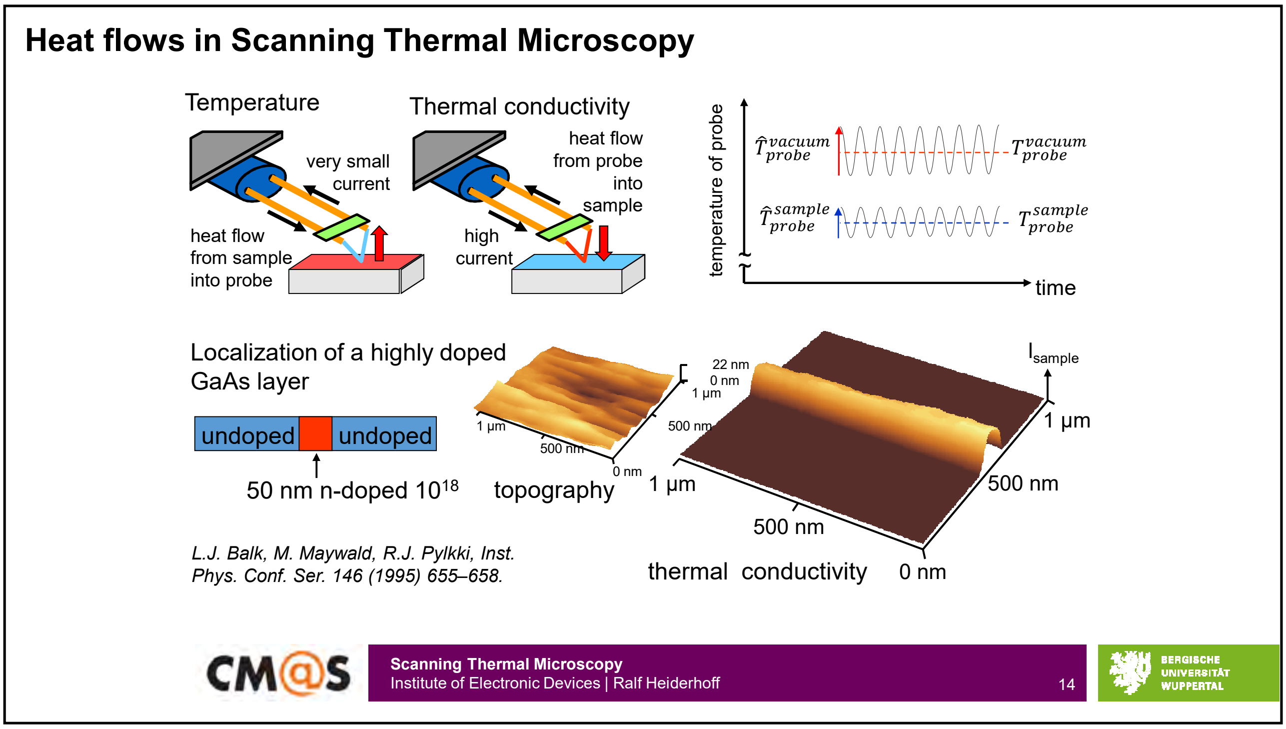

Heat flows in Scanning Thermal Microscopy

L.J. Balk, M. Maywald, R.J. Pylkki, Inst. Phys. Conf. Ser. 146 (1995) 655–658.

Motivation and Purpose


infinitepowersolutions.com

thin film batteries


solarenergyfactsblog.com/

flexible solar cells

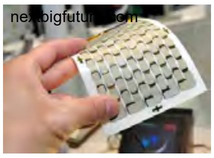
nextbigfuture.com

bendable thermoelectrics

Performances/efficiencies are significantly influenced by thermal properties
(reliability, life time, thermoelectric figure of merit, etc.)

➡ Investigations of cross-plane and in-plane thermal transports in dependence on thin film thicknesses

---

Scanning Thermal Microscopy on thin films

A. Makris et al., RSC Advances, (2016) 6, 94193–94199.

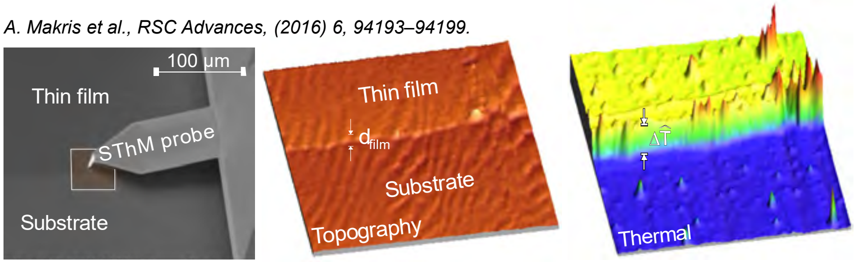

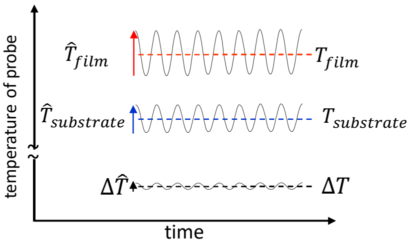

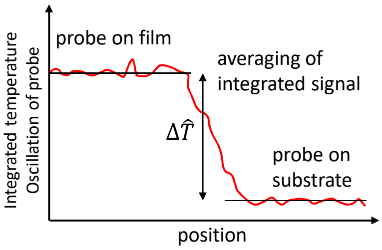

Out-of-plane heat transport

*Si substrate λ_{Si}: 150 $Wm^{-1}K^{-1}$
Al_2O_3 films λ_{Al2O3}: 0.8 $Wm^{-1}K^{-1}$
**Λ_{Al2O3}: 0.47–3.5 nm

*DETHERM, (2017) http://www.dechema.de/Detherm.html
**N. Oka et al., Thin Solid Films, (2010) 518, 3119–3121

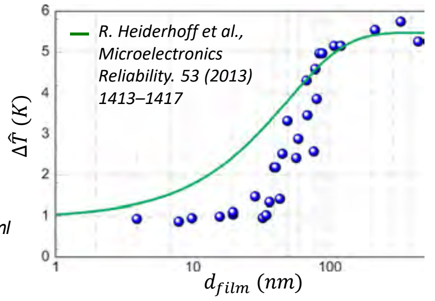

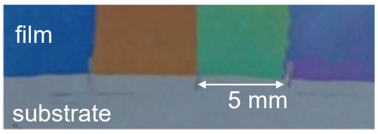

optical image of fabricated step-like film matrix

$$^{***}\ \Delta\hat{T}(d_{film} \ll w) = \frac{\hat{P}}{w \cdot \lambda_{film}} \cdot d_{film},\ \ \mathrm{w} = 2 \cdot r_{contact}$$

$$\Delta\hat{T}(d_{film}) = \frac{\hat{P}}{\lambda_{film}} \cdot \left(1 - e^{-\frac{d_{film}}{2 \cdot r_{contact}}}\right) + \hat{\mathrm{T}}_{contact}$$

⇨ enhanced out-of-plane heat dissipation

***S.-M. Lee and D. G. Cahill, Journal of Applied Physics, (1997) 81, 2590–2595

Stefan-Boltzmann-like heat transport

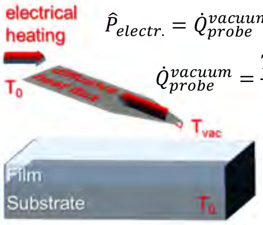

$$\hat{P}_{electr.} = \dot{Q}_{probe}^{vacuum}$$

$$\dot{Q}_{probe}^{vacuum} = \frac{T_{vac} - T_0}{R_{probe}}$$

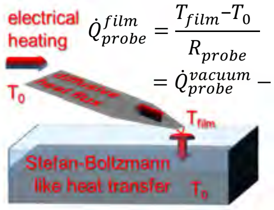

$$\dot{Q}_{probe}^{film} = \frac{T_{film} - T_0}{R_{probe}} = \dot{Q}_{probe}^{vacuum} - \dot{Q}_{Stefan\ Boltzmann}^{*}$$

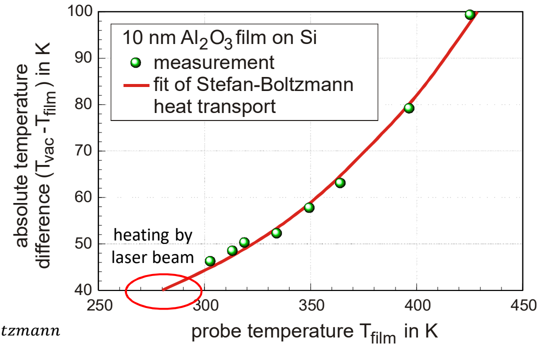

$$\boxed{\frac{T_{vac} - T_{film}}{R_{probe}} = e^{-\frac{d_{film}}{\Lambda_{film}}} \sigma A_{contact}^{Stefan\ Boltzmann} \left(T_{film}^4 - T_0^4\right)}$$

σ: Stefan-Boltzmann constant for phonons
Λ_{film}: phonon mean-free path
$A_{contact}^{Stefan\ Boltzmann}$: effective contact area for ballistic heat transport

*A. Majumdar, Journal of Heat Transfer, (1993) 115, 7–16

In-plane heat transport

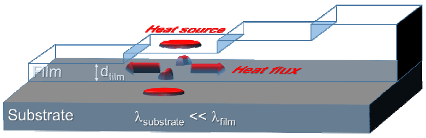

*glass substrate λ_{glass}: 0.8-1.4 $Wm^{-1}K^{-1}$
**TiO_2 films λ_{TiO2}: 2-8 $Wm^{-1}K^{-1}$
***Λ_{TiO2}: 0.4 –1 nm

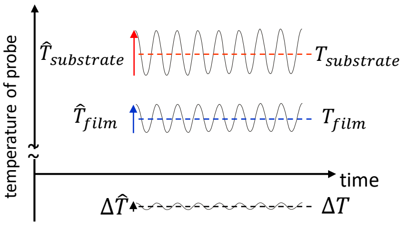

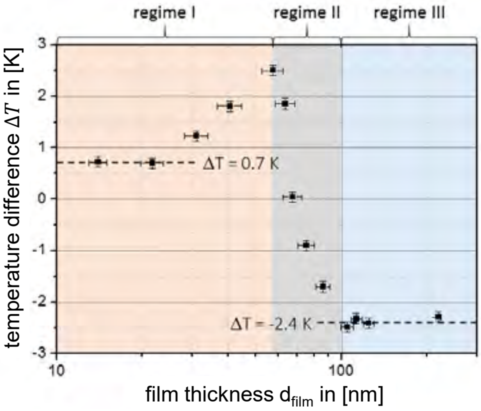

*DETHERM, (2017) http://www.dechema.de/Detherm.html.
**D.J. Kim et al., Int. J. of Thermophysics, (2004) 25, 281–289.
***C. B. Carter, M. G. Norton, in Ceramic Materials, (2013), 641–657

In-plane heat transport

Heiderhoff R. et al., Microelectronics Reliability (2017), doi: 10.1016/j.microrel.2017.06.064

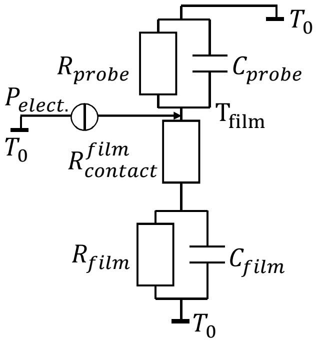

TiO$_2$ layer considered as bulk material in case of d_{film} > 100 nm

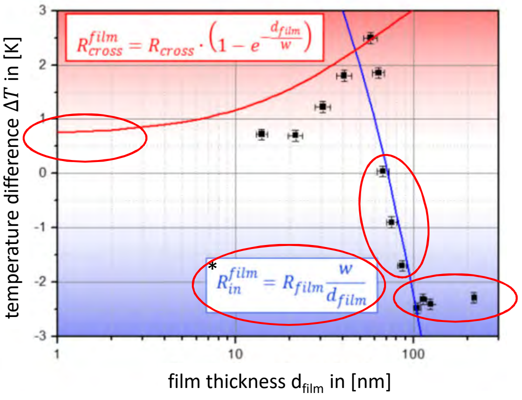

*D. Chu et al. Journal of Vacuum Science & Technology B: Microelectronics and Nanometer Structures, (2001) 19, 2874

Disparate anisotropic heat transport

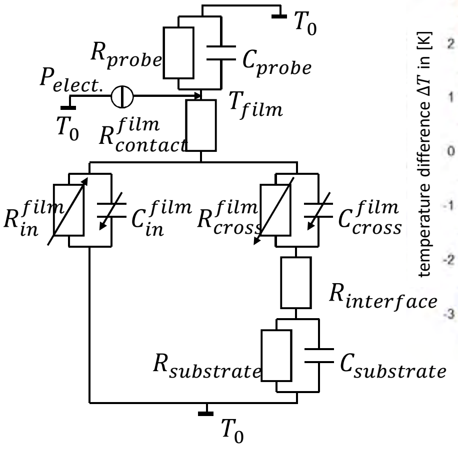

for d_{film} < 100 nm

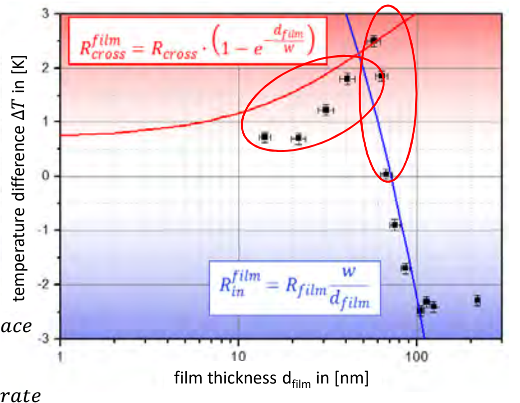

significant out-of-plane Stefan-Boltzmann-like heat dissipation by ballistic thermal phonon transport

significant reduction of the thermal conductivity due to phonon scattering

A.M. Marconnet et al., Journal of Heat Transfer, (2013) 135, doi:10.1115/1.4023577

Frequency dependence of 3ω-method

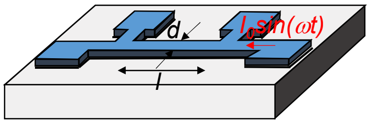

*D. G. Cahill, Review of Scientific Instruments, 1990, **61**, 802–808*

wave number $k = \sqrt{\frac{\omega}{2a}}$

thermal diffusivity: a = $^{\lambda}/_{\rho c}$

$1/k$ >> d : ω_{max} << 2a/d²

$1/k$ < l: ω_{min} > 2a/l²

temperature distribution of line heat source with thermal penetration depth $\frac{1}{\alpha}$ (approximation):

$$\hat{T} = \frac{\hat{P}}{l \cdot \pi \cdot \lambda} \cdot J_0\left(\sqrt{j\alpha r}\right) = \frac{\hat{P}}{l \cdot \pi \cdot \lambda} \cdot \left(\underbrace{\ln(2) - 0.5772 - \frac{j\pi}{4} + \frac{1}{2}\ln\left(\frac{a}{r^2}\right) - \frac{1}{2}\ln(\omega)}_{\text{quantities to be insert in SI without units!}}\right)$$

analysis in the frequency domain

$$\frac{\hat{U}_{3\omega_1} - \hat{U}_{3\omega_2}}{\ln(\omega_1) - \ln(\omega_2)} = \frac{\hat{P}}{l \cdot \pi \cdot \lambda} \cdot \frac{1}{4} I_0 \cdot \frac{dR}{dT}$$

Validation of 3ω-method

FEM model of thermal probe:

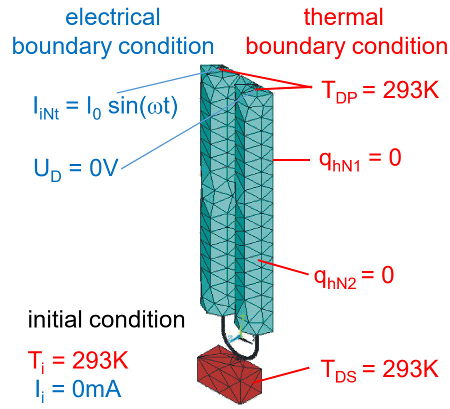

Altes A. et al.: Journal of Physics D: Applied Physics, 37 (2004), issue 6, pp 952 - 963

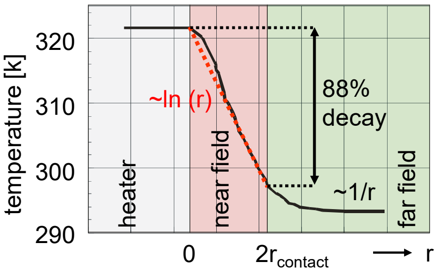

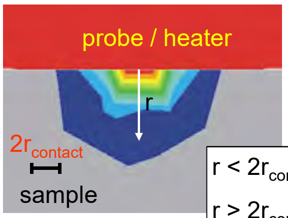

$r < 2r_{contact}$: ~ ln (r)

$r > 2r_{contact}$: ~ 1/r

Validation of 3ω-method

Near field condition of thermal probe:

*Altes A. et al.: Journal of Physics D: Applied Physics, **37** (2004), issue 6, pp 952 - 963*

New approach of estimation

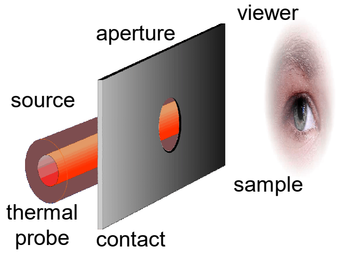

Conventional estimation

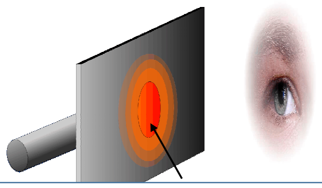

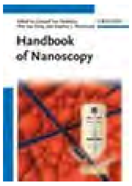

Heiderhoff R. and Balk L.J., "Scanning Probe Microscopy-History, Background, and State of the Art", in Handbook of Nanoscopy (Wiley) 2012

temperature distribution and frequencies depend on probe characteristic

! *S. Gomès et al., Phys. Status Solidi A **212**, No. 3, 477*

Set-up of Scanning Thermal Microscope

P. Tovee et al.; Journal of Applied Physics, (2012) 112, 114317

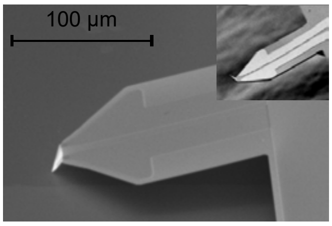

Altes A. et al.: Journal of Physics D: Applied Physics, (2004) 37, 6, 952 - 963

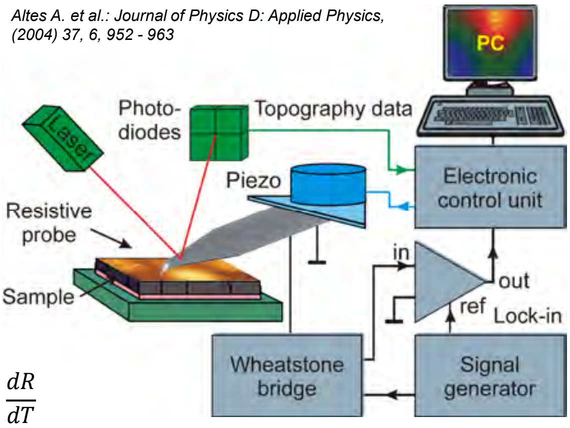

$$\frac{\hat{U}_{3\omega_1}-\hat{U}_{3\omega_2}}{\ln(\omega_1)-\ln(\omega_2)}=\frac{\hat{P}}{l\cdot\pi\cdot\lambda}\cdot\frac{1}{4}I_0\cdot\frac{dR}{dT}$$

D. G. Cahill, Review of Scientific Instruments, (1990) 61, 802–808

S. Lefèvre, S. Volz, Rev. Sci. Instrum. 76 (2005) 033701
S. Gomès et al., Phys. Status Solidi A (2015) 212, 3, 477–494.

Quantitative thermal conductivity analysis on doped areas

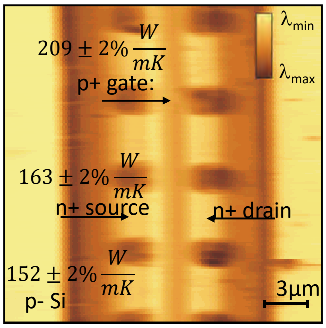

n-MOSFET

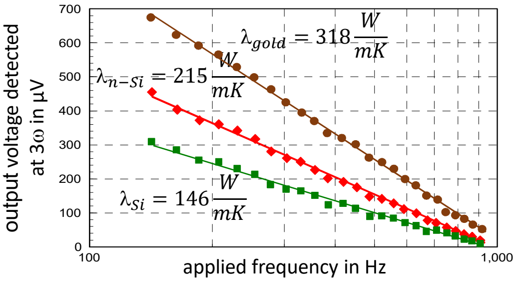

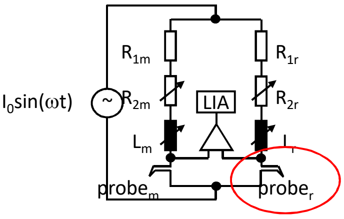

T.H. Lee et al., 27th Int. Symp. Test. Fail. Anal., 2001: pp. 191–197

Thermal conductivity distribution on active devices

Local thermal conductivity λ(T) analyses on micro-machined thin membrane using 3ω method

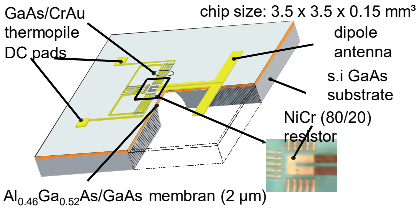

Interface membrane – bulk

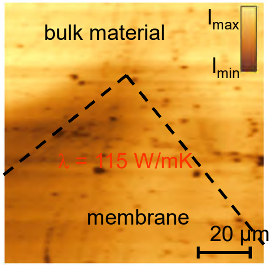

passive termination resistance

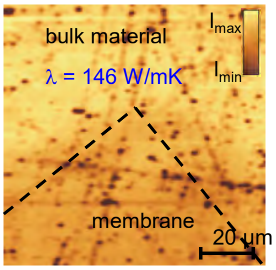

heated termination resistance

A. Altes et al., Superlattices Microstruct. 35 (2004) 465–476

Frequency domain of Scanning Thermal Microscopy

Electrical 3ω-signal generation:

*D. G. Cahill, Review of Scientific Instruments, 1990, **61**, 802–808*

$T(t) \longrightarrow R(t)$

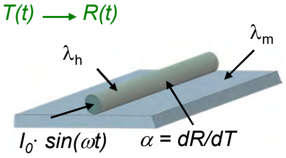

$$R(t) = R_0 - dR/dT \cdot \hat{T}/2 \cdot \cos(2\omega t-\varphi)$$

$$U(t) = I_0 \cdot R_0 \cdot \sin(\omega t) + I_0 \cdot \hat{T}/4 \cdot dR/dT \cdot \sin(\omega t-\varphi)$$
$$- I_0 \cdot \hat{T}/4 \cdot dR/dT \cdot \sin(3\omega t-\varphi)$$

Removal of conductivity information and impact of tip−sample thermal resistance from temperature measurements

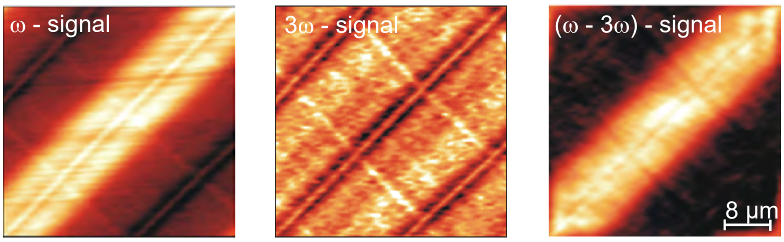

see also: A. Reihani et al., ACS Nano, 2021, doi:10.1021/acsnano.1c08513

Scanning Thermal Microscopy on active devices

Local thermal conductivity analyses on a InGaAlP-LED under different biasing conditions:

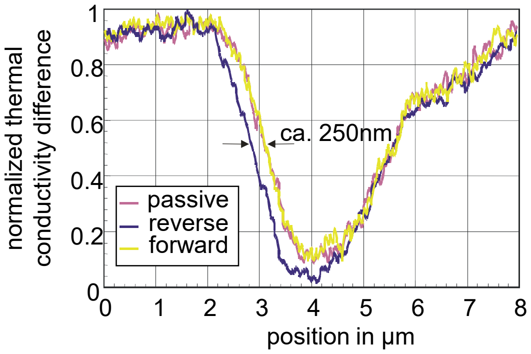

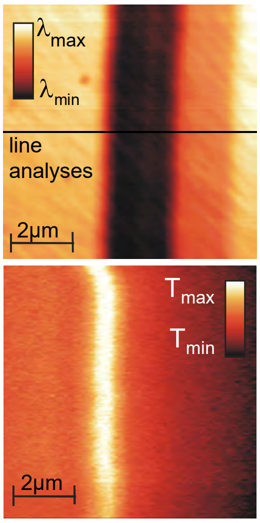

R. Heiderhoff et al., J. Phys. Low Dimens. Struct. 1/2 (2004) 63–70

Motivation and Purpose

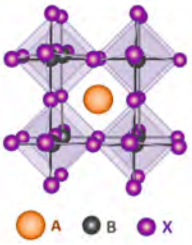

Lev Perovski (1792-1856)

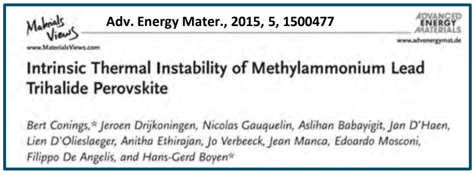

Adv. Energy Mater., 2015, 5, 1500477

Intrinsic Thermal Instability of Methylammonium Lead Trihalide Perovskite

Bert Conings, Jeroen Drijkoningen, Nicolas Gauquelin, Aslihan Babayigit, Jan D'Haen, Lien D'Olieslaeger, Anitha Ethirajan, Jo Verbeeck, Jean Manca, Edoardo Mosconi, Filippo De Angelis, and Hans-Gerd Boyen**

cation A =

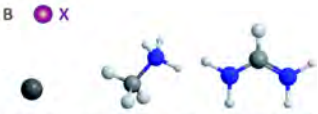

Caesium Methylammonium Formamidinium

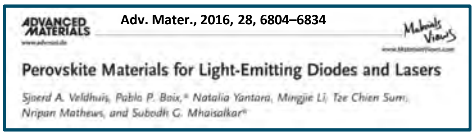

Adv. Mater., 2016, 28, 6804–6834

Perovskite Materials for Light-Emitting Diodes and Lasers

Sjoerd A. Veldhuis, Pablo P. Boix, Natalia Yantara, Mingjie Li, Tze Chien Sum, Nripan Mathews, and Subodh G. Mhaisalkar**

B = Pb, Cd, Ti, or Sn

anion X = I, Br, or Cl

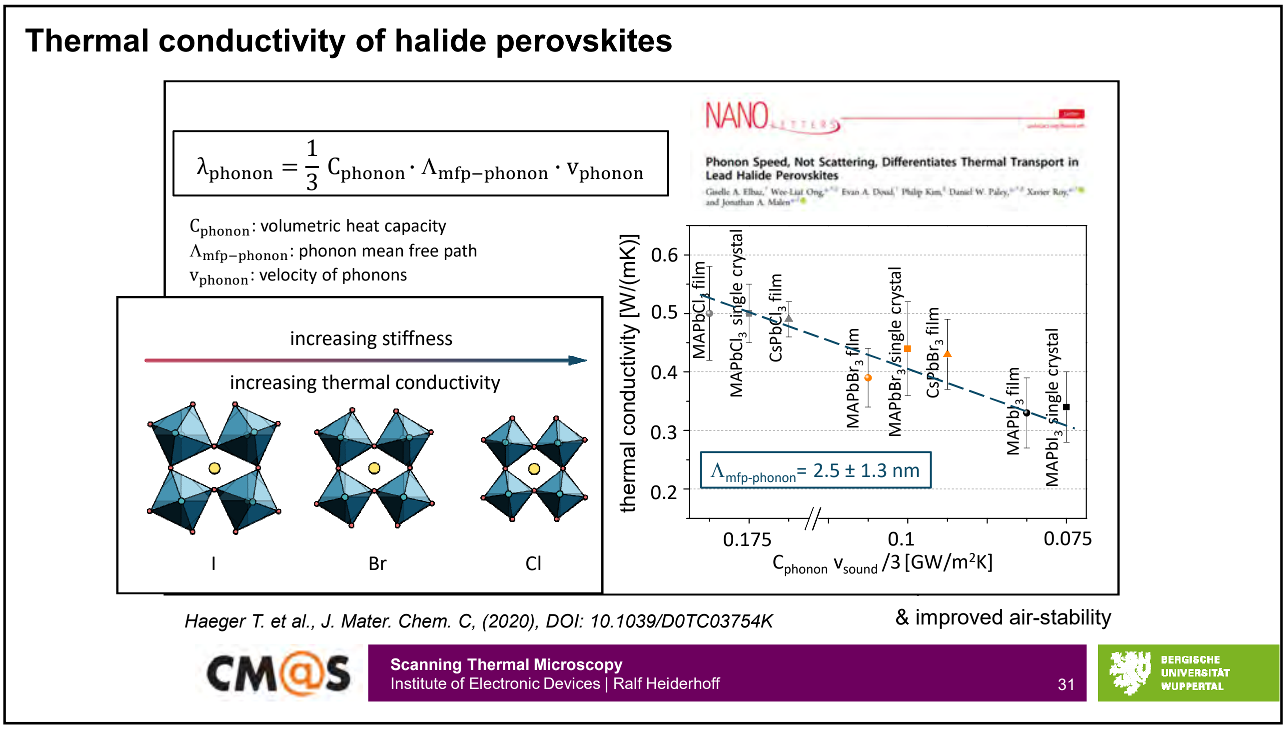

Thermal conductivity of halide perovskites

$$\lambda_{\text{phonon}} = \frac{1}{3} C_{\text{phonon}} \cdot \Lambda_{\text{mfp-phonon}} \cdot v_{\text{phonon}}$$

C_{phonon}: volumetric heat capacity
$\Lambda_{\text{mfp-phonon}}$: phonon mean free path
v_{phonon}: velocity of phonons

NANO LETTERS

Phonon Speed, Not Scattering, Differentiates Thermal Transport in Lead Halide Perovskites

Giselle A. Elbaz, Wee-Liat Ong, Evan A. Doud, Philip Kim, Daniel W. Paley, Xavier Roy, and Jonathan A. Malen

Haeger T. et al., J. Mater. Chem. C, (2020), DOI: 10.1039/D0TC03754K

& improved air-stability

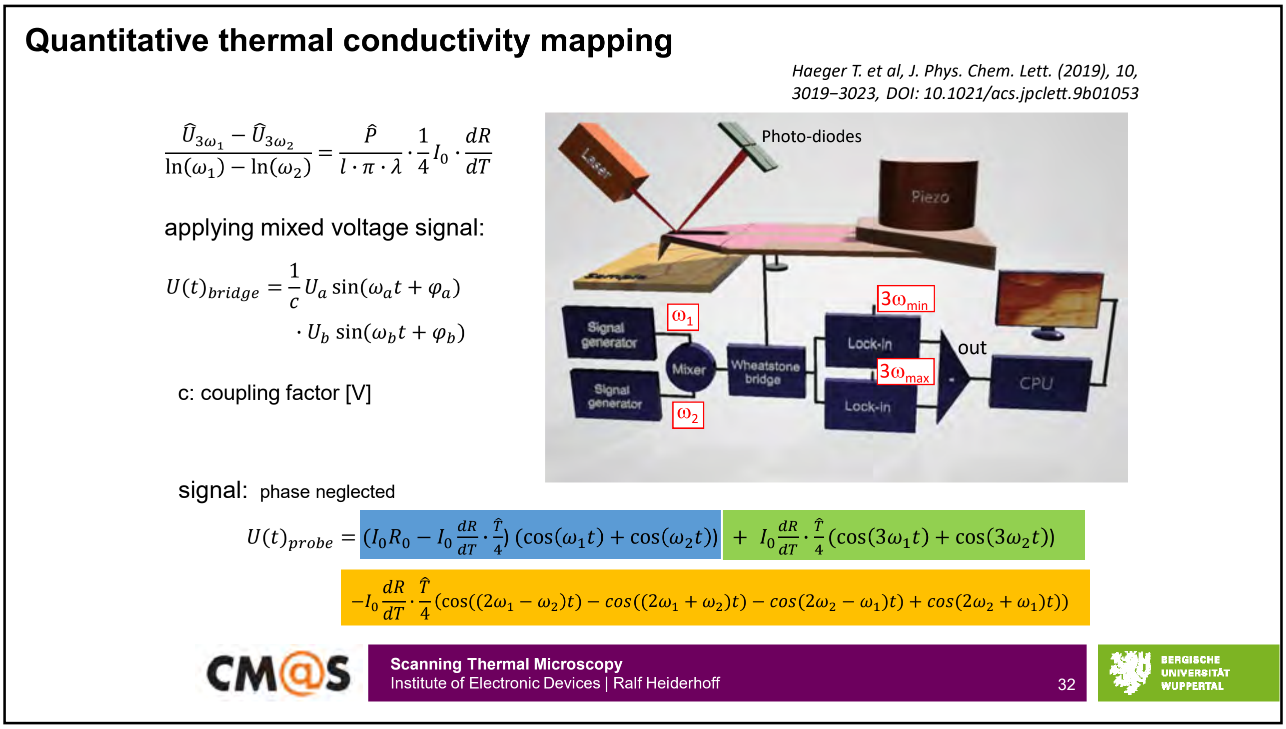

Quantitative thermal conductivity mapping

Haeger T. et al, J. Phys. Chem. Lett. (2019), 10, 3019–3023, DOI: 10.1021/acs.jpclett.9b01053

$$\frac{\hat{U}_{3\omega_1} - \hat{U}_{3\omega_2}}{\ln(\omega_1) - \ln(\omega_2)} = \frac{\hat{P}}{l \cdot \pi \cdot \lambda} \cdot \frac{1}{4} I_0 \cdot \frac{dR}{dT}$$

applying mixed voltage signal:

$$U(t)_{bridge} = \frac{1}{c} U_a \sin(\omega_a t + \varphi_a) \cdot U_b \sin(\omega_b t + \varphi_b)$$

c: coupling factor [V]

signal: phase neglected

$$U(t)_{probe} = \left(I_0 R_0 - I_0 \frac{dR}{dT} \cdot \frac{\hat{T}}{4}\right) (\cos(\omega_1 t) + \cos(\omega_2 t)) + I_0 \frac{dR}{dT} \cdot \frac{\hat{T}}{4} (\cos(3\omega_1 t) + \cos(3\omega_2 t))$$

$$-I_0 \frac{dR}{dT} \cdot \frac{\hat{T}}{4} (\cos((2\omega_1 - \omega_2)t) - cos((2\omega_1 + \omega_2)t) - cos(2\omega_2 - \omega_1)t) + cos(2\omega_2 + \omega_1)t))$$

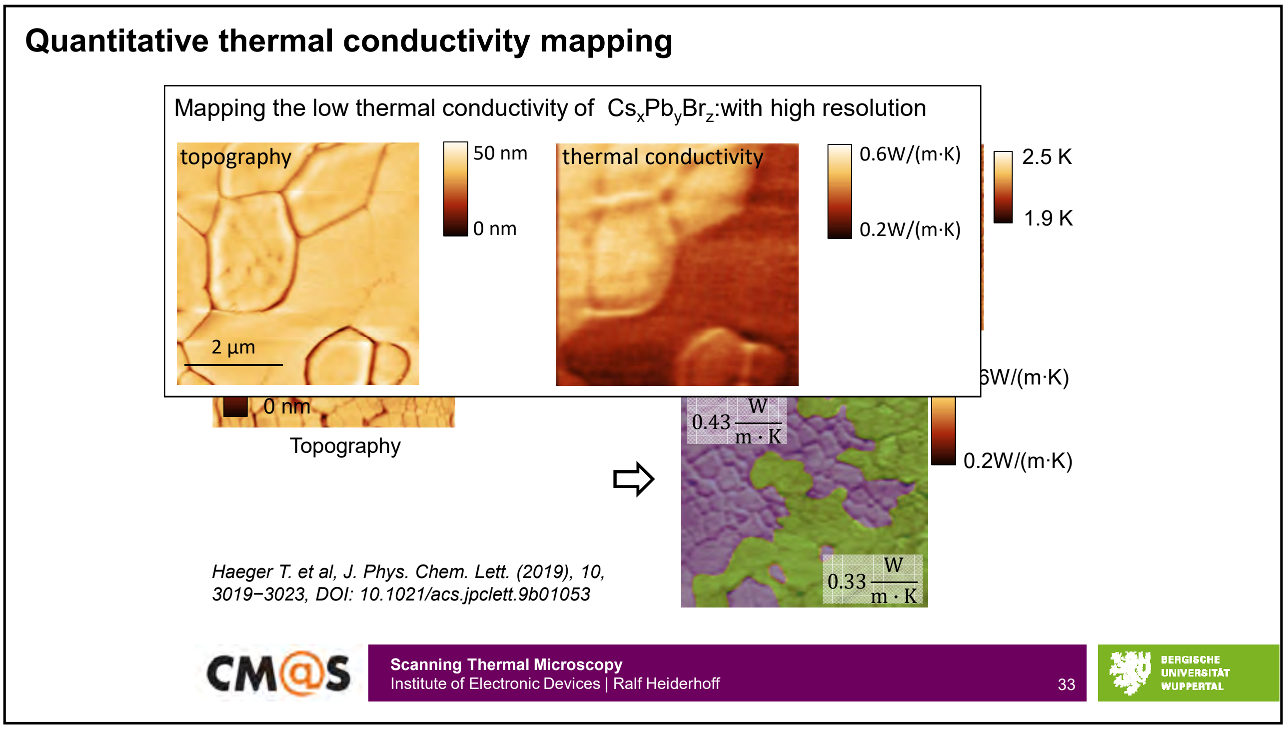

Quantitative thermal conductivity mapping

Mapping the low thermal conductivity of $Cs_xPb_yBr_z$:with high resolution

Haeger T. et al, J. Phys. Chem. Lett. (2019), 10, 3019−3023, DOI: 10.1021/acs.jpclett.9b01053

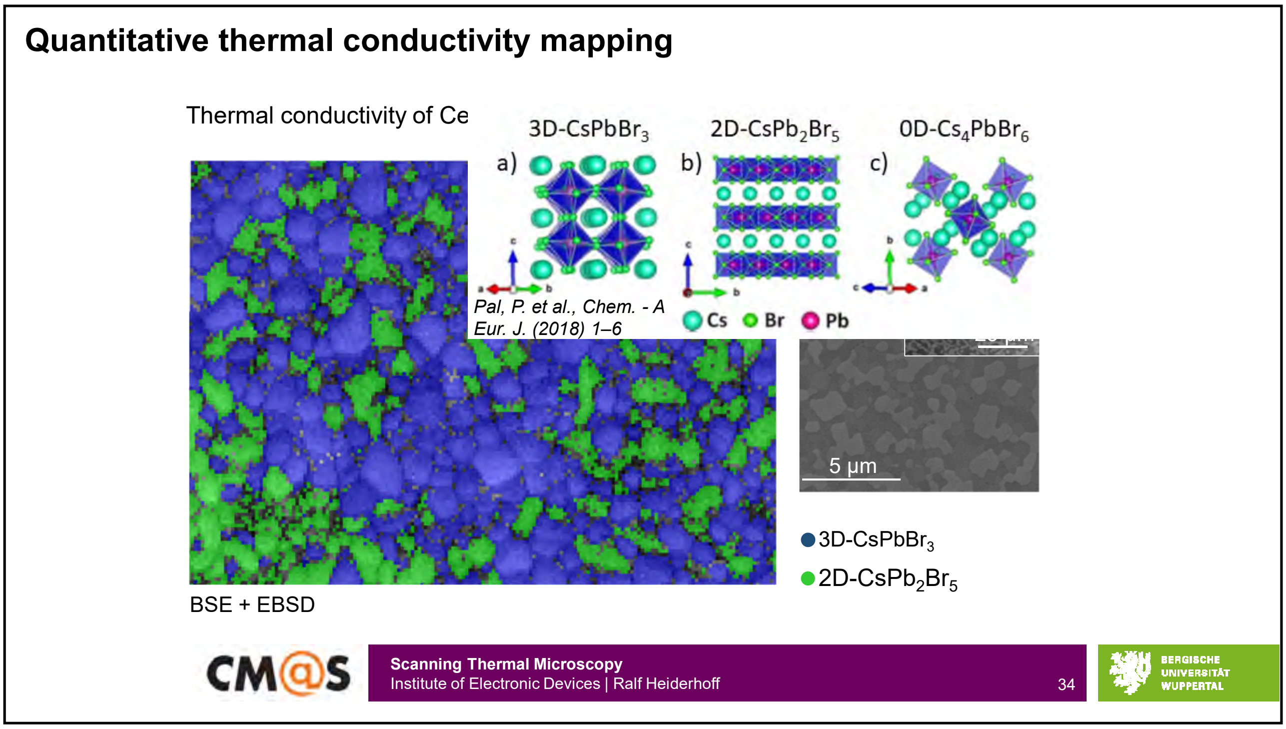

Quantitative thermal conductivity mapping

Thermal conductivity of Ce

Pal, P. et al., Chem. - A Eur. J. (2018) 1–6

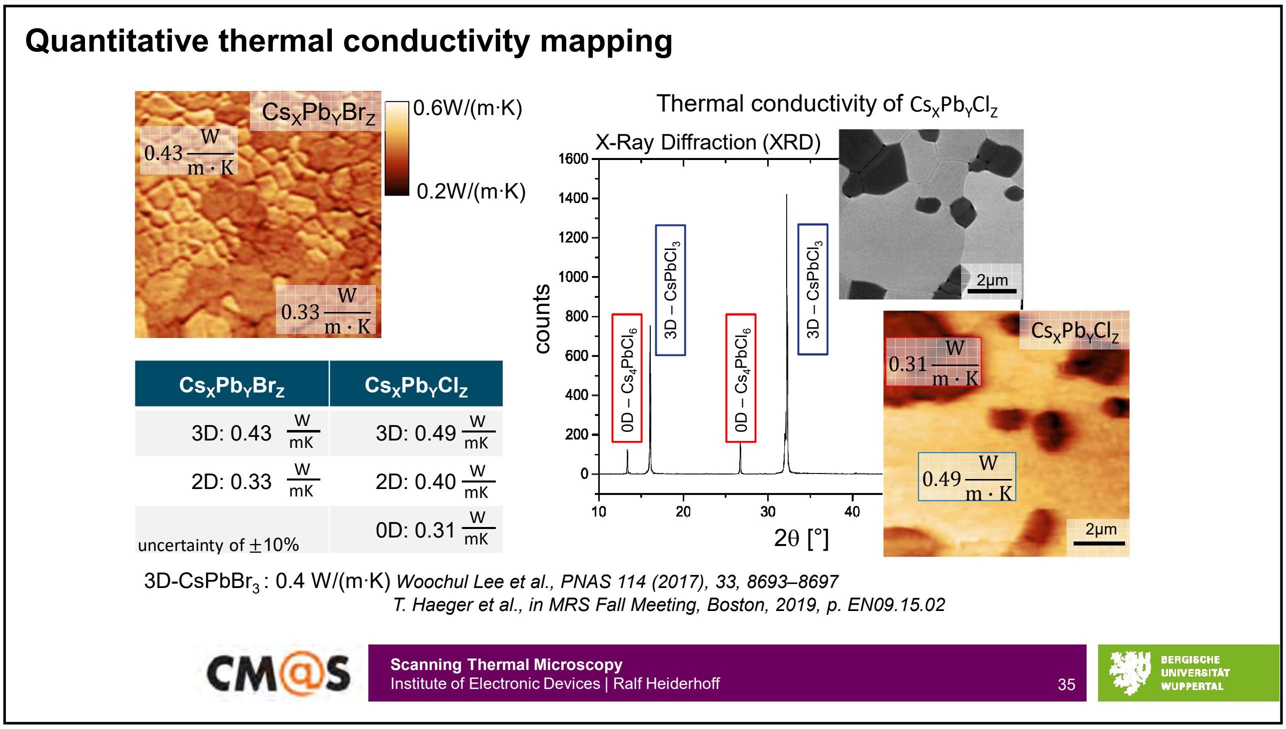

Quantitative thermal conductivity mapping

$Cs_XPb_YBr_Z$	$Cs_XPb_YCl_Z$
3D: 0.43 $\frac{W}{mK}$	3D: 0.49 $\frac{W}{mK}$
2D: 0.33 $\frac{W}{mK}$	2D: 0.40 $\frac{W}{mK}$
uncertainty of ±10%	0D: 0.31 $\frac{W}{mK}$

3D-$CsPbBr_3$: 0.4 W/(m·K) *Woochul Lee et al., PNAS 114 (2017), 33, 8693–8697*
T. Haeger et al., in MRS Fall Meeting, Boston, 2019, p. EN09.15.02

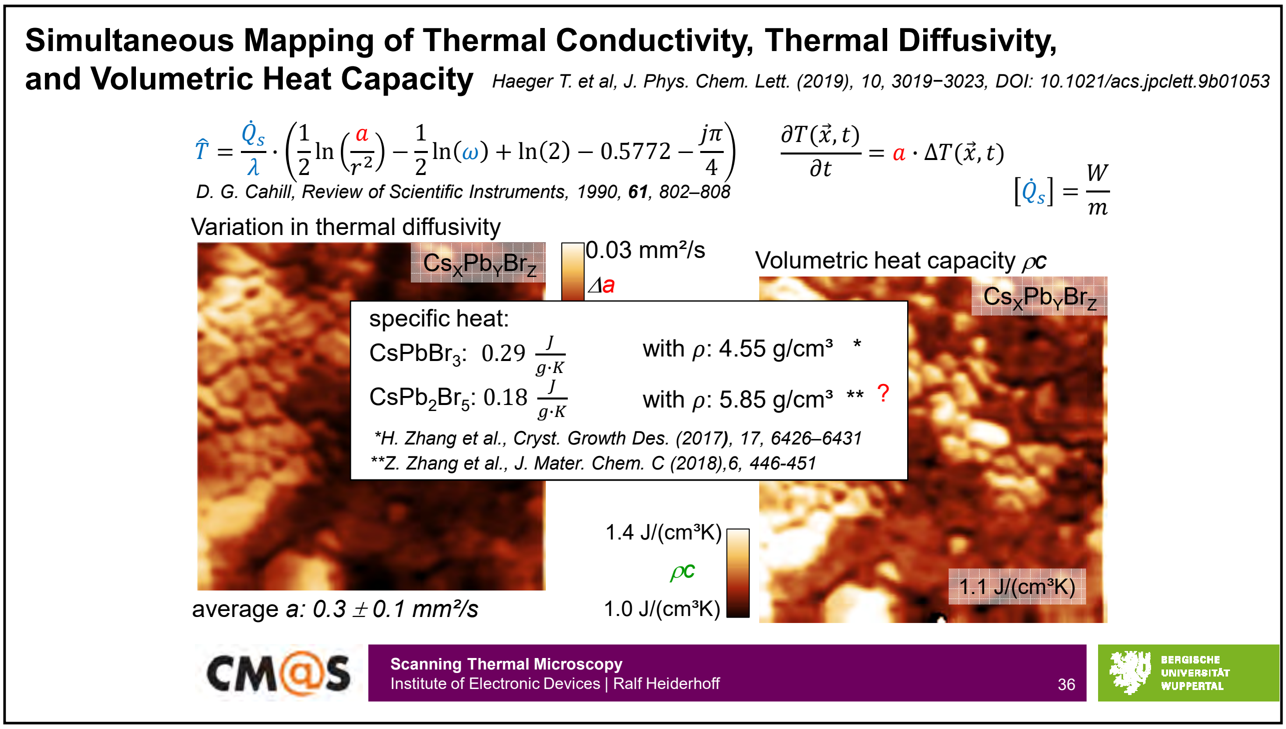

Simultaneous Mapping of Thermal Conductivity, Thermal Diffusivity, and Volumetric Heat Capacity

Haeger T. et al, J. Phys. Chem. Lett. (2019), 10, 3019−3023, DOI: 10.1021/acs.jpclett.9b01053

$$\hat{T} = \frac{\dot{Q}_s}{\lambda} \cdot \left(\frac{1}{2} \ln\left(\frac{a}{r^2}\right) - \frac{1}{2} \ln(\omega) + \ln(2) - 0.5772 - \frac{j\pi}{4} \right)$$

*D. G. Cahill, Review of Scientific Instruments, 1990, **61**, 802–808*

$$\frac{\partial T(\vec{x},t)}{\partial t} = a \cdot \Delta T(\vec{x},t)$$

$$[\dot{Q}_s] = \frac{W}{m}$$

Variation in thermal diffusivity

Volumetric heat capacity ρc

specific heat:
$CsPbBr_3$: $0.29 \frac{J}{g \cdot K}$ with ρ: 4.55 g/cm³ *
$CsPb_2Br_5$: $0.18 \frac{J}{g \cdot K}$ with ρ: 5.85 g/cm³ ** ?
**H. Zhang et al., Cryst. Growth Des. (2017), 17, 6426–6431*
***Z. Zhang et al., J. Mater. Chem. C (2018),6, 446-451*

average *a: 0.3 ± 0.1 mm²/s*

Simultaneous Mapping of Thermal Conductivity, Thermal Diffusivity, and Volumetric Heat Capacity

Haeger T. et al, J. Phys. Chem. Lett. (2019), 10, 3019−3023, DOI: 10.1021/acs.jpclett.9b01053

$$\hat{T} = \frac{\dot{Q}_s}{\lambda} \cdot \left(\frac{1}{2} \ln\left(\frac{a}{r^2}\right) - \frac{1}{2} \ln(\omega) + \ln(2) - 0.5772 - \frac{j\pi}{4} \right) \qquad \frac{\partial T(\vec{x},t)}{\partial t} = a \cdot \Delta T(\vec{x},t)$$

$[\dot{Q}\ ] = \frac{W}{m}$

D. C

Var

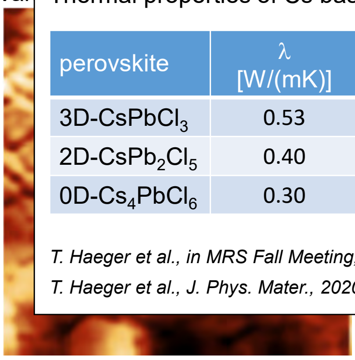

Thermal properties of Cs based chloride perovskites

perovskite	λ [W/(mK)]	a [mm²/s]	c_v [J/(cm³K)]
3D-$CsPbCl_3$	0.53	0.5	1.1
2D-$CsPb_2Cl_5$	0.40	0.6	0.7
0D-Cs_4PbCl_6	0.30	0.5	0.5

T. Haeger et al., in MRS Fall Meeting, Boston, 2019, p. EN09.15.02

T. Haeger et al., J. Phys. Mater., 2020, 3, 024004

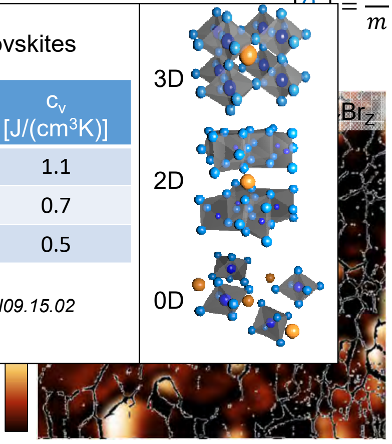

average *a: 0.3 ± 0.1 mm²/s*

Motivation and Purpose

Phase transitions of halide perovskites

T. Haeger et al., J.Mater.Chem.C, 2020, 8, 14289-14311

Adv. Mater., 2016, 28, 6804–6834

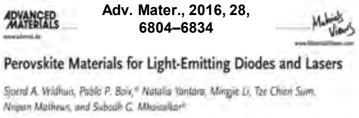

ADVANCED MATERIALS

Perovskite Materials for Light-Emitting Diodes and Lasers

Sjoerd A. Veldhuis, Pablo P. Boix,* Natalia Yantara, Mingjie Li, Tze Chien Sum, Nripan Mathews, and Subodh G. Mhaisalkar*

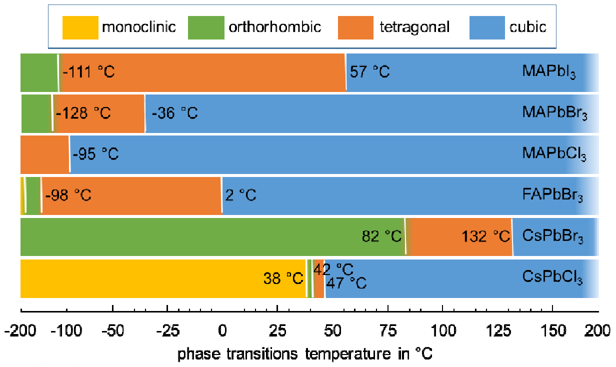

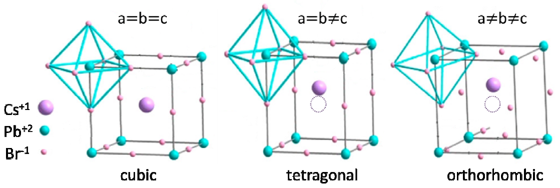

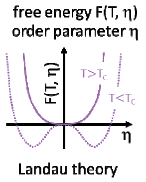

Thermal properties of $CsPbCl_3$ at phase transitions

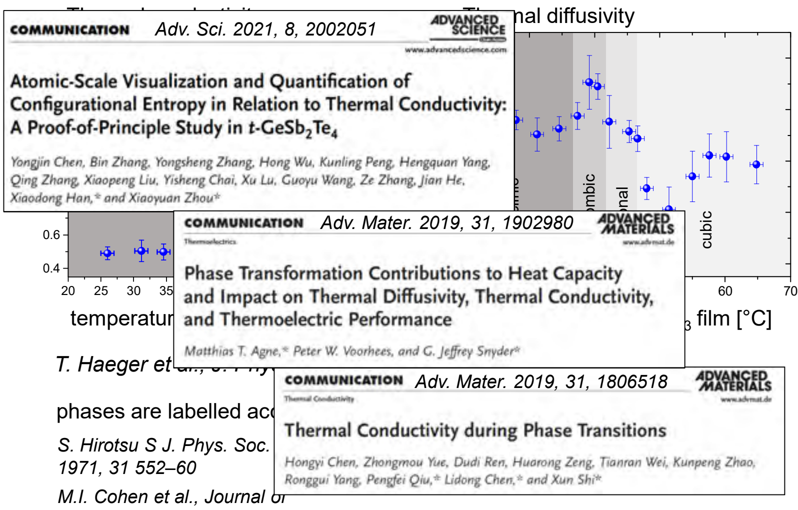

COMMUNICATION *Adv. Sci. 2021, 8, 2002051*

Atomic-Scale Visualization and Quantification of Configurational Entropy in Relation to Thermal Conductivity: A Proof-of-Principle Study in t-$GeSb_2Te_4$

Yongjin Chen, Bin Zhang, Yongsheng Zhang, Hong Wu, Kunling Peng, Hengquan Yang, Qing Zhang, Xiaopeng Liu, Yisheng Chai, Xu Lu, Guoyu Wang, Ze Zhang, Jian He, Xiaodong Han, and Xiaoyuan Zhou**

COMMUNICATION *Adv. Mater. 2019, 31, 1902980*

Phase Transformation Contributions to Heat Capacity and Impact on Thermal Diffusivity, Thermal Conductivity, and Thermoelectric Performance

Matthias T. Agne, Peter W. Voorhees, and G. Jeffrey Snyder**

COMMUNICATION *Adv. Mater. 2019, 31, 1806518*

Thermal Conductivity during Phase Transitions

Hongyi Chen, Zhongmou Yue, Dudi Ren, Huarong Zeng, Tianran Wei, Kunpeng Zhao, Ronggui Yang, Pengfei Qiu, Lidong Chen,* and Xun Shi**

T. Haeger et

phases are labelled acc

S. Hirotsu S J. Phys. Soc. 1971, 31 552–60

M.I. Cohen et al., Journal of Applied Physics 1971, 42, 13

Volumetric heat capacity

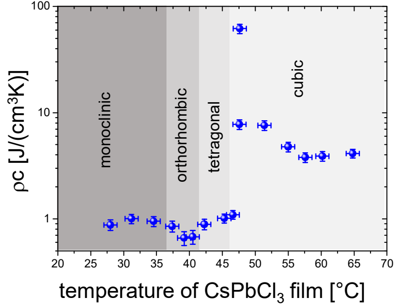

1st order

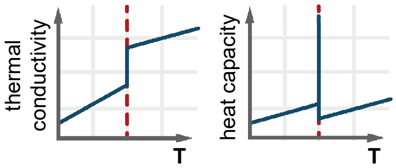

Closing remarks

Thermal and thermoelastic quantities determinable

- on ultra-high und ultra-low thermal conductors
- with spatial resolution in the nanometer range
- with femto-meter sensitivity
- on thin films
- at phase transitions

Scanning near-field thermal microscopy techniques assisted by complementary finite element simulation

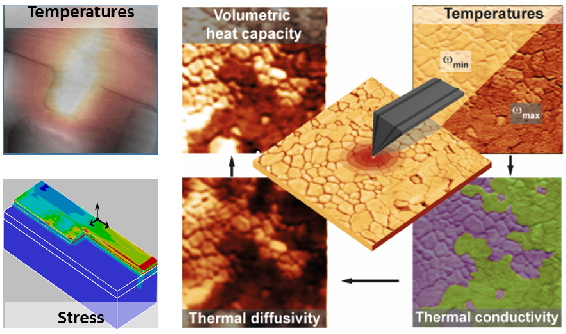

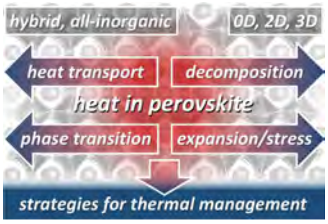

- Reliability investigations on smart materials and devices
- Transition from diffusive heat flux to ballistic Stefan–Boltzmann like heat transport in thin films
- Thermal properties of hybrid and all-inorganic perovskites in dependence on choice of cations & halides, dimensionality, and crystal-phase
  - ultra low thermal conductivities
  - low thermal diffusivities
  - low volumetric heat capacities

Acknowledgments

M. Maywald
G.B.M. Fiege
M. Palaniappan
T.H. Lee
A. Altes
E. Hendarto
A.-K. Geinzer (Tiedemann)
M. Fakhri
K. Kurz
Y.F. Zhang
A. Makris
T. Haeger
K. Dawada
M. Al-Khafaji
M. Wilmes
J. Bahr
M. Ketterer

Prof. Dr. rer. nat. Dr. h.c. (bsuir) Ludwig Josef Balk
Prof. Dr. J.C.H. Phang †
Prof. Dr. Y. Ji / Prof. Dr. X.D. Han

- This work is currently supported by the Deutsche Forschungsgemeinschaft (DFG) under the project number 508311353 (HE 2698/11-1).

Acknowledgments

Thank you for your attention

Scanning Thermal Microscopy
Institute of Electronic Devices | Ralf Heiderhoff